Helicity Transfer in Strong Laser Fields via the Electron Anomalous Magnetic Moment

Yan-Fei Li,[1,*] Yue-Yue Chen,[2,†] Karen Z. Hatsagortsyan,[3] and Christoph H. Keitel[3]
[1]Department of Nuclear Science and Technology, School of Energy and Power Engineering, Xi'an Jiaotong University, Xi'an 710049, China
[2]Department of Physics, Shanghai Normal University, Shanghai 200234, China
[3]Max-Planck-Institut für Kernphysik, Saupfercheckweg 1, 69117 Heidelberg, Germany

(Received 15 November 2021; revised 9 March 2022; accepted 30 March 2022; published 27 April 2022)

Electron beam longitudinal polarization during the interaction with counterpropagating circularly polarized ultraintense laser pulses is investigated, while accounting for the anomalous magnetic moment of the electron. Although it is known that the helicity transfer from the laser photons to the electron beam is suppressed in linear and nonlinear Compton scattering processes, we show that the helicity transfer nevertheless can happen via an intermediate step of the electron radiative transverse polarization, phase matched with the driving field, followed up by spin rotation into the longitudinal direction as induced by the anomalous magnetic moment of the electron. With spin-resolved QED Monte Carlo simulations, we demonstrate the consequent helicity transfer from laser photons to the electron beam with a degree up to 10%, along with an electron radial polarization up to 65% after multiple photon emissions in a femtosecond timescale. This effect is detectable with currently achievable laser facilities, evidencing the role of the leading QED vertex correction to the electron anomalous magnetic moment in the polarization dynamics in ultrastrong laser fields.

DOI: 10.1103/PhysRevLett.128.174801

The development of modern ultraintense laser facilities, with a record intensity already reaching 10^{23} W/cm^2 [1–4], brings about new possibilities for testing predictions of strong-field quantum electrodynamics (QED) theory. The typical field strength characterizing the strong-field QED regime is the Schwinger critical field $E_S = 1.3 \times 10^{16}$ V/cm (corresponding to the intensity of $I_S = 4.6 \times 10^{29}$ W/cm^2) [5,6]. While directly not attainable by lasers, the critical field can be achieved using the Lorentz boost of ultrarelativistic electrons in a head-on collision geometry [7], which enables the experimental study of nonlinear regimes of strong-field QED processes. In particular, recently such experiments are proposed at DESY (LUXE) [8], and at FACET-II (E320) in the Stanford Linear Accelerator Center (SLAC) [9].

In strong background fields electrons can be polarized due to the spin-flip during photon emissions, which was first discovered for synchrotron radiation [10–14] and termed as radiative polarization. Recently, the possibility has been proven of efficient radiative polarization using ultrastrong laser fields, applied to produce polarized electrons [15–17] and positrons [18–20] in a femtosecond timescale, as well as for polarization transfer from electrons to γ rays in laser fields [21,22]. The polarization effects in strong laser fields have a capability of detecting the quantum stochastic nature of electron dynamics [23], diagnosing magnetic fields of plasma [24], and providing ultrashort, high-brilliance, low-emittance polarized beam sources for fundamental studies in high-energy physics [25–27] and material science [28,29]. The completely spin- and photon-polarization-resolved probability rates for nonlinear Compton scattering have been derived from strong-field QED theory in the Furry picture for a plane-wave laser field [30], and for the locally constant fields [31], as well as via the quantum operator method [32], and employed for a deep analysis of all polarization channels, helicity transfer in the perturbative regime, and investigation of the polarization dependent energy and angle distributions [33]. Furthermore, the study of polarization effects has been extended to higher-order QED processes [34–39], and QED cascades [40].

In radiative polarization the electron spin flip is preferable along the instantaneous magnetic field in the rest frame of the electron. Because of that in a storage ring or in ultrastrong laser fields initially unpolarized electrons are mostly polarized transversely after the interaction. Nevertheless, high-precision high-energy physics at accelerators demands longitudinal beam polarization, e.g., the Q_{weak} experiment at Jefferson Lab [41] and E158 at SLAC [42]. Presently, one common way of producing circularly polarized electrons in accelerators is via photoemission induced by a circular polarized laser field from a solid [43,44]. There were a series of attempts to employ Compton scattering for this purpose. While here the helicity of the laser photons is efficiently transferred to emitted γ rays [45,46], the longitudinal polarization of the scattered electrons is not efficient in the linear regime and suppressed in the nonlinear regime. Thus, the electron longitudinal polarization can reach only $P_{\parallel} = \boldsymbol{P} \cdot \boldsymbol{\beta} \sim 10^{-3}$

during a single photon emission in a circularly polarized laser field [47] at the laser strong field parameter $a_0 = 100$ and electron velocity $\boldsymbol{\beta} \sim$ GeV. Moreover, while scattered electrons in the Compton process are weakly polarized, the total longitudinal polarization of the electron beam is vanishing. This is due to the polarization of unscattered electrons, which exactly cancels that of scattered ones [48,49]. The latter is explained as interference of the incoming electron wave function with that of the forward scattered one.

Recently, it has been demonstrated that QED radiative corrections, i.e., the interaction of the electron with its own radiation field, can also affect the electron spin dynamics in intense background fields [35–37]. In particular, due to QED loop corrections, the electrons exact spin-dependent wave function becomes unstable inside a strong background field, leading to 1% polarization for unscattered electrons [35,36]. The latter provides the QED description of the polarization of unscattered electrons discussed in Ref. [48]. The spin effects resulted from the electron mass loop are also described as a spin rotation, which appeared to be more significant within the tail of a tightly focused laser beam [37]. Furthermore, there are experimental plans to reach the fully nonperturbative regime of QED, employing beam-beam collisions in TeV-class lepton colliders [50–55], when the effective field in the rest frame of electrons could be supercritical, and radiative corrections to QED processes nonperturbative and substantial.

In this Letter, we investigate the role of the electrons' anomalous magnetic moment on the helicity transfer from a circularly polarized (CP) laser pulse to an ultrarelativistic electron beam for the nonlinear Compton scattering process in the radiation reaction dominated regime. The electron three-dimensional polarization properties are analyzed using numerical Monte Carlo simulations based on the spin-resolved radiation probabilities in the local constant field approximation (LCFA). While previous studies neglecting the QED radiative corrections came to a conclusion that the helicity transfer from laser photons to electrons is forbidden in the nonlinear Compton scattering process, we obtain a sizable longitudinal polarization of electrons when the one-loop QED vertex correction [11,56] to the anomalous contribution to the magnetic moment is accounted for. A longitudinal polarization degree close to 3% is shown, which could be further improved up to 10% with postselection techniques. Compared with the conventional way via the Sokolov-Ternov effect, our scheme can directly produce substantial longitudinal electron polarization without an additional polarization rotator and in an orders of magnitude faster timescale. More importantly, we prove the scenario of the helicity transfer during nonlinear Compton scattering. Initially, spin flips during photon emissions induce electron transverse polarization which is phase matched with the laser field. Because of the latter property and the anomalous correction to the magnetic moment [57–59], the oscillating transverse polarization is transformed into accumulated longitudinal polarization during the interaction. The latter demonstrates a signature of QED radiative corrections for electron polarization dynamics in ultrastrong laser fields. Additionally, the electron transverse radiative polarization with a degree over 60% is shown after the interaction, of interest for high-energy applications.

We model the laser-electron interaction process with the Monte Carlo method [60–63], which treats the photon emissions quantum mechanically with the spin-resolved photon emission probabilities in the LCFA [15,21]. The LCFA [14,64–68] is valid at $a_0 \equiv |e|E_0/(m\omega_0) \gg 1$, when the coherence length of the photon emission, $l \sim \lambda_L/a_0$, is much smaller than the typical length of the trajectory (here the laser wavelength λ_L). Furthermore, E_0 is the laser field amplitude, ω_0 the laser frequency, and $e(<0)$, m are the electron charge and mass, respectively. Relativistic units $\hbar = c = 1$ are used throughout. The photon emission probability is determined by the local value of the quantum strong-field parameter $\chi_e \equiv |e|\sqrt{-(F_{\mu\nu}p^\nu)^2}/m^3$, where $F_{\mu\nu}$ is the field tensor and p^ν the four vector of electron momentum. The simulation method is the following [69]: The common statistical event generator is conducted at each simulation step to determine whether or not a photon-emission occurs based on the photon emission probability via the Baier-Katkov QED operator method [70]. If a photon-emission occurs, the emitted photon energy is determined by the stochastic procedure and spectral probability with polarization involved, while the electron and photon polarizations via the averaged algorithm involving the density matrix for the mixed state of an electron ensemble [63,71,72] to reduce the statistical fluctuation. Because of the radiation reaction, the electron momentum is reduced to $\boldsymbol{p}_f \approx (1 - \omega_\gamma/|\boldsymbol{p}_i|)\boldsymbol{p}_i$, where $\boldsymbol{p}_{i,f}$ are the electron momentum before and after emission, respectively, and ω_γ the energy of emitted photon. If the photon-emission event is rejected, the electron spin changes according to the nonradiation probability [18,63]. This no-emission spin variation originates from the radiative correction of the one-loop propagator correction where the electron propagator is modified by the process that a virtual photon is emitted and reabsorbed by the electron [35]. At first order in the fine-structure constant α, it cancels the longitudinal polarization of the electrons induced by emitting soft photons in a circularly polarized field [38,48,73]. In the regime $a_0 \sim 1$, the cancellation is broken after including radiation reaction, leading to a nonzero longitudinal polarization of the final electrons [39].

The spin precession between photon emissions is governed by the Thomas-Bargmann-Michel-Telegdi equation [74,75]: $d\mathbf{S}/dt = \boldsymbol{S} \times \boldsymbol{F}$, with

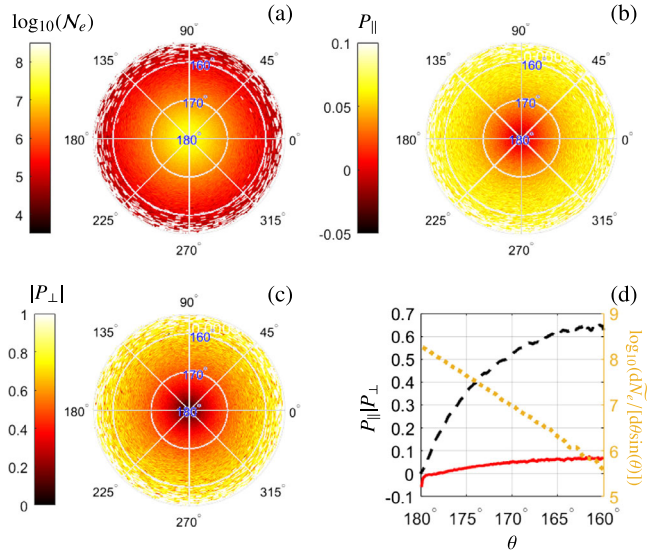

FIG. 1. (a) Distribution of electron number density $\log_{10}(\mathcal{N}_e)$, with $\mathcal{N}_e = dN_e/[d\varphi d\sin\theta d\theta d\phi]$. (b) Average longitudinal polarization $P_\parallel = \boldsymbol{\beta}\cdot\boldsymbol{S}_f$. (c) Average transverse polarization $|P_\perp| = |\boldsymbol{S}_f - \boldsymbol{\beta}\cdot\boldsymbol{S}_f|$, vs polar angle θ in [155°,180°] and the azimuthal angle of φ in [0°,360°], respectively. (d) $P_\parallel$ (red-solid), $P_\perp$ (black-dashed), and $\log_{10}(dN_e/[d\theta\sin(\theta)])$ (yellow-dotted) at $\varphi = 180°$ vs θ, respectively.

$$\boldsymbol{F} = \frac{e}{m}\left[-\left(\frac{g}{2}-1\right)\frac{\gamma}{\gamma+1}(\boldsymbol{\beta}\cdot\mathbf{B})\boldsymbol{\beta} + \left(\frac{g}{2}-1+\frac{1}{\gamma}\right)\mathbf{B} - \left(\frac{g}{2}-\frac{\gamma}{\gamma+1}\right)\boldsymbol{\beta}\times\mathbf{E}\right], \quad (1)$$

where $\mathbf{E}$ and $\mathbf{B}$ are the laser electric and magnetic fields, respectively, $\beta \approx -1$ the electron velocity, and g the electron gyromagnetic factor. Taking into account the radiative correction to the first order of α in the interaction with the radiation field and being exact with respect to the external field [12],

$$g(\chi_e) = 2 + 2\mu(\chi_e), \quad \mu(\chi_e) = \frac{\alpha}{\pi\chi_e}\int_0^\infty \frac{y}{(1+y)^3}\mathbf{L}_{\frac{1}{3}}\left(\frac{2y}{3\chi_e}\right)dy, \quad (2)$$

with $\mathbf{L}_{\frac{1}{3}}(z) = \int_0^\infty \sin\{(3z/2)[x+(x^3/3)]\}dx$. At $\chi_e \ll 1$, one obtains the Schwinger result $g = 2 + (\alpha/\pi) \approx 2.00232$. The electron dynamics is described by the Newton equation with the Lorentz force. The modification of the equation of motion due to the anomalous magnetic moment [76,77] does not change the electron dynamics [69].

The polarization effect of electrons is illustrated in Fig. 1. A right-hand CP tightly focused Gaussian laser pulse is used [78], with peak intensity $I_0 \approx 2\times10^{22}$ W/cm^2 ($a_0 = 100\sqrt{2}$), pulse duration (FWHM) $\tau = 5T_0$, with the laser period T_0, $\lambda = 1$ μm, and focal radius $w_0 = 5\lambda$. The counterpropagating cylindrical electron bunch has a length of $L_e = 5\lambda$ and radius of $w_e = 1\lambda$. $N_e = 10^6$ unpolarized electrons are distributed longitudinally uniformly. The transverse distribution is Gaussian with the variance of $\sigma_{x,y} = 0.3\lambda$. The initial electron kinetic energy is $\varepsilon_0 = 1$ GeV, the energy spread $\Delta\varepsilon_0/\varepsilon_0 = 10\%$, and the angular divergence (FWHM) $\Delta\theta = 0.1$ mrad. The diagrammatic detailed setup (see Fig. 17 in the Supplemental Material [69]) and the feasibility for larger beam spreadings is shown in Ref. [69]. As the quantum parameter for pair creation $\bar{\chi}_\gamma \equiv |e|\sqrt{-(F_{\mu\nu}k^\nu)^2/m^3} \approx 0.005 \ll 1$, with $k^\mu = (\omega, \boldsymbol{k})$ being the four-momentum of laser photons, the rate of producing e^+e^- pairs by emitted photons is $W_{\rm pair} \sim 10^{-5}$ and consequently can be neglected [69].

After the interaction the scattered electrons concentrate in the center of the angle distribution, and have longitudinal, as well as transverse polarization, see Figs. 1(a)–1(c). The average longitudinal polarization degree is not large $\bar{P}_\parallel = (1/N_e)\sum_{i=1}^{N_e}\boldsymbol{S}_i\cdot(\boldsymbol{\beta}_i/|\boldsymbol{\beta}_i|) \approx 2.65\%$, nevertheless exceeding by an order of magnitude the QED tree-level result $\bar{P}_\parallel \approx 0.1\%$ [47]. The electrons are highly polarized in the transverse plane with polarization vector pointing to the center of the beam. The electron number density decreases exponentially from the center to the peripheries [Fig. 1(d)], while the polarization $P_\parallel$ and $P_\perp$ increase with the deflection angle. Therefore, the polarization purity can be increased by selecting large angle electrons with post-momentum-angle selection techniques. Meanwhile, the longitudinal polarization degree can be increased by post-energy selection due to the $P_\parallel$ dependency on the electrons energy (Fig. 2). Higher $P_\parallel$ can be obtained by collecting low energy electrons. For instance, by collecting the electrons with energies less than 45 MeV, we can get a polarization degree of $P_\parallel = 10\%$ with the percentage of number of 1%.

The reason for the electron beam polarization is analyzed in Fig. 3. Without radiation reaction, the electrons typically move along a spiral trajectory in the CP laser pulse, with the transverse momentum perpendicular to the electric field [Figs. 3(a) and 3(b)]. In each time step, the spin vector of an electron flips to the direction parallel or antiparallel to the

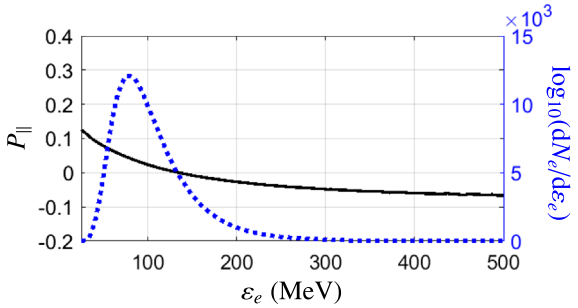

FIG. 2. Longitudinal polarization $P_\parallel$, and number density $\log_{10}(dN_e/d\varepsilon_e)$ (MeV^{-1}), versus final electron energy ε_e.

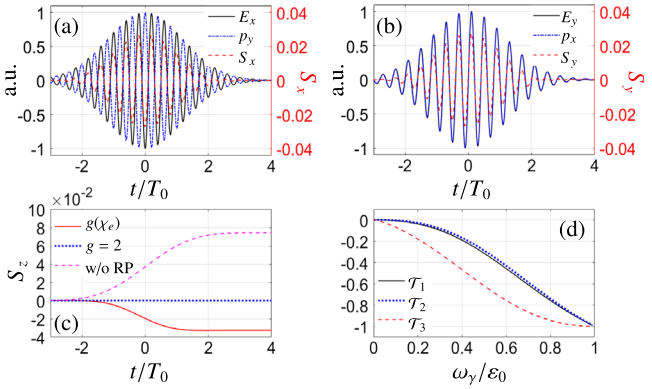

FIG. 3. The evolution of the field and electron parameters: (a) E_x, p_y, and S_x; (b) E_y, p_x, and S_y; (c) S_z for $g = g(\chi_e)$ (red solid), $g = 2$ (blue dotted), and $g = g(\chi_e)$ but without radiative polarization (magenta dashed), for an initially unpolarized electron beam. The electron spin dynamics is calculated numerically with Eq. (3). At $t = 0$ the peak of the laser pulse reaches the focal spot. The field and momentum components are normalized to their maximum. Radiation reaction for the electron momenta is neglected for simplicity [80]. (d) The values of the three terms in Eq. (5) are defined as $\mathcal{T}_1 = (1/a)\{u^2\mathrm{K}_{2/3} - u\mathrm{K}_{1/3}[\boldsymbol{S}_i \cdot (\boldsymbol{\beta}\times\boldsymbol{s})]\}$, $\mathcal{T}_2 = (1/a)\{u^2\mathrm{IntK}_{1/3} - u\mathrm{K}_{1/3}[\boldsymbol{S}_i \cdot (\boldsymbol{\beta}\times\boldsymbol{s})]\}$, and $\mathcal{T}_3 = (1/a)u(1+u)\mathrm{K}_{1/3}(\boldsymbol{\beta}\times\boldsymbol{s})$, with $a = (1+u)\mathrm{IntK}_{1/3} - (2+2u+u^2)\mathrm{K}_{2/3} + \boldsymbol{S}_i \cdot (\boldsymbol{\beta}\times\boldsymbol{s})u\mathrm{K}_{1/3}$ and $S_i = 0.01$, $\boldsymbol{S}_i$ is parallel to $(\boldsymbol{\beta}\times\boldsymbol{s})$.

instantaneous spin quantization axis according to the quantum probabilities [18]. The evolution of polarization of an electron ensemble including both effects of spin flip and spin precession is described by the following equation [12]:

$$\frac{d\boldsymbol{S}}{dt} = \boldsymbol{S}\times\boldsymbol{F} - \frac{\alpha m}{\sqrt{3}\pi\gamma}\int_0^\infty \frac{u^2 du}{(1+u)^3}[\mathrm{K}_{2/3}\boldsymbol{S} + (\mathrm{IntK}_{1/3} - \mathrm{K}_{2/3})(\boldsymbol{S}\cdot\boldsymbol{\beta})\boldsymbol{\beta} + (\boldsymbol{\beta}\times\boldsymbol{a})\mathrm{K}_{1/3}], \quad (3)$$

where $\mathrm{IntK}_{\frac{1}{3}} \equiv \int_{u'}^\infty dz\mathrm{K}_{\frac{1}{3}}(z)$, $\mathrm{K}_{2/3} = \mathrm{K}_{2/3}(u')$, $\mathrm{K}_{1/3} = \mathrm{K}_{1/3}(u')$, and K_n is the nth-order modified Bessel function of the second kind, $u' = 2u/3\chi_e$, $u = \omega_\gamma/(\varepsilon_0 - \omega_\gamma)$, and ε_0 the electron energy, ω_γ the photon energy, and $\boldsymbol{a} = \dot{\boldsymbol{\beta}}/|\dot{\boldsymbol{\beta}}|$. As shown in Figs. 3(a)–3(c), the transverse polarization $\boldsymbol{S}_\perp$ oscillates synchronously with $\boldsymbol{E}$, and $|S_z|$ builds up exponentially. The phase matching between $S_{x,y}$ and $E_{x,y}$ follows from the domination of the last term in Eq. (3) for $\boldsymbol{S}_\perp$. In fact, $\mathrm{K}_{2/3}|\boldsymbol{S}_\perp| \ll \mathrm{K}_{1/3}$, and the spin precession role [first term in Eq. (3)] is known to be minor for the transverse radiative polarization. Consequently, $d\boldsymbol{S}_\perp/dt$ is parallel to $-\boldsymbol{\beta}\times\boldsymbol{a}$, and thus, $\boldsymbol{S}_\perp$ is parallel to $\boldsymbol{E}$. We analyze the accumulation of the longitudinal polarization:

$$\frac{dS_\parallel}{dt} = -\frac{e}{m}\boldsymbol{S}_\perp \cdot \left[\left(\frac{g}{2}-1\right)\boldsymbol{\beta}\times\mathbf{B} + \left(\frac{g\beta}{2} - \frac{1}{\beta}\right)\mathbf{E}\right] - \frac{\alpha m}{\sqrt{3}\pi\gamma}S_\parallel\int_0^\infty \frac{u^2 du}{(1+u)^3}\mathrm{IntK}_{1/3}, \quad (4)$$

with the use of Eq. (11.171) in Ref. [7]. For an initially unpolarized electrons beam, the longitudinal polarization arises due to the $\boldsymbol{S}_\perp$ term, connected to the spin procession, which can be approximated as $dS_\parallel/dt \approx -(2e/m)[(g/2)-1]\boldsymbol{S}_\perp \cdot \mathbf{E}$, taking account of $S^i_\parallel = 0$, $\beta \approx 1$ and $\boldsymbol{\beta}\parallel -\boldsymbol{k}$. As well known, the Dirac theory predicts precisely $g = 2$, which leads to vanishing longitudinal polarization [Fig. 3(c)]. However, the QED loop corrections induce an anomalous contribution to the electron's magnetic moment, $g \neq 2$ [Eq. (2)], which results in rotation of the transverse polarization to longitudinal direction in the case when $\boldsymbol{S}_\perp$ and $\boldsymbol{E}$ are phase matched. Note that, the phase matching of $\boldsymbol{S}_\perp$ and $\boldsymbol{E}$ is a unique feature of electrons in a counter-propagating circularly polarized laser field, and, consequently, such a configuration is essential for producing $P_\parallel$ [69]. Therefore, the electron anomalous magnetic moment is the origin of helicity transfer. Our estimation of $\boldsymbol{S}_\parallel$ via Eq. (3) yields $P_\parallel = 3.26\%$ after the interaction, which is in accordance with the simulation result. Thus, even though the spin precession is trivial for the well-studied transverse polarization in strong-field QED [12,15,16], it plays an essential role in generating longitudinal polarization. The correlation between anomalous magnetic moment and longitudinal polarization may consequently provide new potential of accurately measuring $g/2 - 1$. For instance, the maximum and the changing rate of the averaged polarization degree exclusively depend on the anomalous magnetic moment, which would be sensitive measures of the anomaly $g/2 - 1$ [79].

Moreover, the Monte Carlo simulation reveals a radial polarization feature of the electron beam with absolute value $P_\perp$ up to 65% [Fig. 1(c)]. Even though the averaged transverse polarization is negligible due to the cancellation from opposite angles, which coincides with the prediction of modified BMT equations [Figs. 3(a) and 3(b)], it is possible to collect electrons in a certain angle to obtain a high transverse polarization, as well as a high longitudinal polarization by applying a spin-rotating system [15]. We can give a simple estimation of the radial polarization using the spin-flip transition probabilities, which determine the spin change after a photon emission [15,18]:

$$\Delta\boldsymbol{S}^R = \frac{[u^2\mathrm{K}_{2/3} - u\mathrm{K}_{1/3}[\boldsymbol{S}_i\cdot(\boldsymbol{\beta}\times\boldsymbol{a})]]\boldsymbol{S}_\perp + [u^2\mathrm{IntK}_{1/3} - u\mathrm{K}_{1/3}[\boldsymbol{S}_i\cdot(\boldsymbol{\beta}\times\boldsymbol{a})]]\boldsymbol{S}_\parallel + u(1+u)\mathrm{K}_{1/3}(\boldsymbol{\beta}\times\boldsymbol{a})}{(1+u)\mathrm{IntK}_{1/3} - (2+2u+u^2)\mathrm{K}_{2/3} + \boldsymbol{S}_i\cdot(\boldsymbol{\beta}\times\boldsymbol{a})u\mathrm{K}_{1/3}}. \quad (5)$$

The initial spin $\boldsymbol{S}_i$ is taken as the average polarization of the ensemble shown in Figs. 3(a)–3(c), i.e., $|\boldsymbol{P}_\perp| \sim 10^{-2}$ and $|\boldsymbol{P}_\parallel| \sim 10^{-2}$. In this case, the fist two terms of Eq. (5) are negligible compared with the last term since $|\boldsymbol{S}| \ll 1$, and the remaining terms with modified Bessel functions are comparable, see Fig. 3(d). Consequently, the change of transverse spin is estimated as $\Delta \boldsymbol{S}_\perp^R \propto -\boldsymbol{\beta} \times \boldsymbol{a}$, antiparallel to the momentum of the scattered electron after one photon emission [69]. This feature is preserved during multiple photon emissions, yielding the radial transverse electron polarization [Fig. 1(c)].

Since the transverse polarization $|\Delta \boldsymbol{S}_\perp^R|$ increases with the emitted photon energy [69], the electrons that experience more energy loss obtain higher transverse polarization, which subsequently contributes to higher longitudinal polarization according to Eq. (4). Meanwhile, as the deflection angle of electron $\theta_D \sim 1/\gamma$, the transverse polarization degree increases with the decrease of θ [Fig. 1(d)]. Therefore, $P_\parallel$ is inversely proportional to ε_e and θ [Figs. 1(d) and 2]. The above analysis is not relevant for scattered electrons with energy higher than 135 MeV, corresponding to those within angle of $\theta > 167°$. These electrons are polarized opposite to the laser helicity and the polarization degree increases with ε_e and θ [Fig. 2]. This counterintuitive polarization feature highlights two different contributions of QED loop effects to the electron polarization in background fields. First, the loop effects induce anomalous magnetic moment $g > 2$, which yields the rotation of the radiative transverse polarization into the longitudinal direction. Second, the loop effects result in varying the electron spin even without photon emissions [35]. The latter effect is included in our Monte Carlo simulations by means of an additional no-photon-emission probability for the spin-flip [63]. We estimate this effect via turning off artificially the photon emission in the modified BMT equation [69]:

$$\frac{d\boldsymbol{S}^{NR}}{dt} = \frac{e}{m}[\boldsymbol{S} \times \boldsymbol{F}] - \frac{\alpha m}{\sqrt{3}\pi\gamma}\int_0^\infty \frac{du}{(1+u)^3}\{[\boldsymbol{S}\cdot(\boldsymbol{\beta}\times\boldsymbol{a})\, u\mathrm{K}_{1/3}]\boldsymbol{S} - (\boldsymbol{\beta}\times\boldsymbol{a})u\mathrm{K}_{1/3}\}. \tag{6}$$

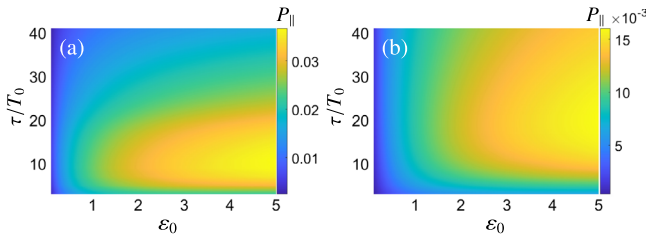

FIG. 4. The dependence of the longitudinal polarization $P_\parallel$ on the laser duration τ and the initial electron energy ε_0 at the laser intensity of $a_0 = 100\sqrt{2}$ and $50\sqrt{2}$, respectively.

Compared with Eq. (3), the dominant term $(\boldsymbol{\beta} \times \boldsymbol{a})$ has opposite sign. Thus, if the transverse spin dynamics is governed by no-emission polarization, the phase of $\boldsymbol{S}_\perp$ is opposite to $\boldsymbol{E}$. Consequently, the energetic electrons obtain a negative longitudinal polarization [Fig. 3(c)] due to polarization rotation associated with anomalous magnetic moment, i.e., $P_\parallel = -P_z \propto \mathbf{S}_\perp \cdot \mathbf{E} < 0$, which is opposite to the low-energy electrons in the remaining contribution to the spectrum, as shown in Fig. 2.

The impacts of the laser and electron beam parameters on the longitudinal polarization are analyzed in Fig. 4. With the increase of ε_0 and a_0, the transverse polarization $P_\perp$ increases since radiative polarization is enhanced for a larger radiation loss scaled by $\chi_e \approx 5 \times 10^{-6} a_0 \gamma$, and consequently, the longitudinal polarization $P_\parallel$ grows. While for a certain ε_0 and a_0, $P_\parallel$ rises at first and then declines with respect to τ. Without radiation reaction, one would expect a monotonously increase of $P_\parallel$ with the increase of interaction time from Eq. (3). Unfortunately, radiation reaction breaks the phase correlation between $\boldsymbol{S}_\perp$ and $\boldsymbol{E}$, and disrupts the longitudinal polarization built at the preliminary stage of the interaction, resulting in the decrease of $P_\parallel$ for a long laser pulse [69].

Concluding, we have analyzed the role of the anomalous magnetic moment and no-photon-emission spin dynamics, i.e., effects which both are consequences of QED radiative corrections, for electron polarization in the radiation dominated regime with multiple photon emissions. We showed that exclusively due to these effects helicity transfer is possible from CP laser photons to electrons in ultrastrong field regime $a_0 \gg 1$, which challenged the belief that circularly polarized laser beams cannot induce high longitudinal polarization. Thanks to high collision luminosity in the nonlinear regime, this single-shot signature is robust with respect to the laser and electron parameters and measurable with currently available experimental technology [69]. It could also serve for testing QED predictions on radiative corrections.

The authors thank Y.-T. Li, W.-M. Wang, and Q.-Z. Lv for helpful discussions. This work is supported by the National Natural Science Foundation of China (Grants No. 12075187 and No. 12074262), the Strategic Priority Research Program of the Chinese Academy of Sciences (Grant No. XDA25031000), the National Key R&D Program of China (Grant No. 2021YFA1601700), and the Shanghai Rising-Star Program.

*liyanfei@xjtu.edu.cn
†yueyuechen@shnu.edu.cn

[1] J. W. Yoon, Y. G. Kim, I. W. Choi, J. H. Sung, H. W. Lee, S. K. Lee, and C. H. Nam, Realization of laser intensity over 10^{23} W/cm^2, Optica **8**, 630 (2021).

[2] LLNL, ELI-Beamlines Reach deal to ramp up L3-HAPLS performance, https://lasers.llnl.gov/news/llnl-eli-beamlines-reach-deal-ramp-up-l3-hapls-performance.

[3] B. Rus, P. Bakule, D. Kramer, G. Korn, J. T. Green, J. Nóvak, M. Fibrich, F. Batysta, J. Thoma, J. Naylon *et al.*, ELI-beamlines laser systems: Status and design options, Proc. SPIE Int. Soc. Opt. Eng. **8780**, 87801T (2013).

[4] J. Kawanaka, K. Tsubakimoto, H. Yoshida, K. Fujioka, Y. Fujimoto, S. Tokita, T. Jitsuno, N. Miyanaga, and G.-E. D. Team, Conceptual design of sub-exa-watt system by using optical parametric chirped pulse amplification, J. Phys. Conf. Ser. **688**, 012044 (2016).

[5] J. Schwinger, On gauge invariance and vacuum polarization, Phys. Rev. **82**, 664 (1951).

[6] A. Di Piazza, C. Müller, K. Z. Hatsagortsyan, and C. H. Keitel, Extremely high-intensity laser interactions with fundamental quantum systems, Rev. Mod. Phys. **84**, 1177 (2012).

[7] J. D. Jackson, *Classical Electrodynamics*, 3rd ed. (Wiley, Hoboken, NJ, 1999).

[8] H. Abramowicz, M. Altarelli, R. Aßmann, T. Behnke, Y. Benhammou, O. Borysov, M. Borysova, R. Brinkmann, F. Burkart, K. Büßer *et al.*, Letter of intent for the luxe experiment, arXiv:1909.00860.

[9] The FACET-II SFQED Collaboration, Probing strong-field QED at FACET-II (SLAC E-320) (unpublished).

[10] A. A. Sokolov and I. M. Ternov, On polarization and spin effects in the theory of synchrotron radiation, Sov. Phys. Dokl. **8**, 1203 (1964).

[11] V. N. Baier, V. M. Katkov, and V. M. Strakhovenko, Radiative effects in an external electromagnetic field, Sov. Phys.-Dokl. **16**, 230 (1971).

[12] V. N. Baĭer, Radiative polarization of electrons in storage rings, Sov. Phys. Usp. **14**, 695 (1972).

[13] Y. Derbenev and A. M. Kondratenko, Polarization kinematics of particles in storage rings, Zh. Èksper. Teoret. Fiz. **64**, 1918 (1973) [Sov. Phys . JETP **37**, 968 (1973)], http://jetp.ras.ru/cgi-bin/dn/e_037_06_0968.pdf.

[14] V. N. Baier, V. M. Katkov, and V. M. Strakhovenko, *Electromagnetic Processes at High Energies in Oriented Single Crystals* (World Scientific, Singapore, 1998).

[15] Y.-F. Li, R. Shaisultanov, K. Z. Hatsagortsyan, F. Wan, C. H. Keitel, and J.-X. Li, Ultrarelativistic Electron-Beam Polarization in Single-Shot Interaction with an Ultraintense Laser Pulse, Phys. Rev. Lett. **122**, 154801 (2019).

[16] D. Seipt, D. Del Sorbo, C. P. Ridgers, and A. G. R. Thomas, Ultrafast polarization of an electron beam in an intense bichromatic laser field, Phys. Rev. A **100**, 061402(R) (2019).

[17] H.-H. Song, W.-M. Wang, J.-X. Li, Y.-F. Li, and Y.-T. Li, Spin-polarization effects of an ultrarelativistic electron beam in an ultraintense two-color laser pulse, Phys. Rev. A **100**, 033407 (2019).

[18] Y.-F. Li, Y.-Y. Chen, W.-M. Wang, and H.-S. Hu, Production of Highly Polarized Positron Beams via Helicity Transfer from Polarized Electrons in a Strong Laser Field, Phys. Rev. Lett. **125**, 044802 (2020).

[19] Y.-Y. Chen, P.-L. He, R. Shaisultanov, K. Z. Hatsagortsyan, and C. H. Keitel, Polarized Positron Beams via Intense Two-Color Laser Pulses, Phys. Rev. Lett. **123**, 174801 (2019).

[20] F. Wan, R. Shaisultanov, Y.-F. Li, K. Z. Hatsagortsyan, C. H. Keitel, and J.-X. Li, Ultrarelativistic polarized positron jets via collision of electron and ultraintense laser beams, Phys. Lett. B **800**, 135120 (2020).

[21] Y.-F. Li, R. Shaisultanov, Y.-Y. Chen, F. Wan, K. Z. Hatsagortsyan, C. H. Keitel, and J.-X. Li, Polarized Ultrashort Brilliant Multi-GeV γ Rays via Single-Shot Laser-Electron Interaction, Phys. Rev. Lett. **124**, 014801 (2020).

[22] S. Tang, B. King, and H. Hu, Highly polarised gamma photons from electron-laser collisions, Phys. Lett. B **809**, 135701 (2020).

[23] R.-T. Guo, Y. Wang, R. Shaisultanov, F. Wan, Z.-F. Xu, Y.-Y. Chen, K. Z. Hatsagortsyan, and J.-X. Li, Stochasticity in radiative polarization of ultrarelativistic electrons in an ultrastrong laser pulse, Phys. Rev. Research **2**, 033483 (2020).

[24] Z. Gong, K. Z. Hatsagortsyan, and C. H. Keitel, Retrieving Transient Magnetic Fields of Ultrarelativistic Laser Plasma via Ejected Electron Polarization, Phys. Rev. Lett. **127**, 165002 (2021).

[25] G. Moortgat-Pick *et al.*, Polarized positrons and electrons at the linear collider, Phys. Rep. **460**, 131 (2008).

[26] A. V. Subashiev, Yu. A. Mamaev, Yu. P. Yashin, J. E. Clendenin, and , Spin polarized electrons: Generation and applications, Phys. Low Dimens. Struct. **1**, 1 (1999), [SLAC PUB 8035 (1998)].

[27] L. Elouadrhiri, T. A. Forest, J. Grames, W. Melnitchouk, and E. Voutier, Proceedings of the international workshop on positrons at Jefferson Lab, AIP Conf. Proc. **1160**, 13 (2009), https://aip.scitation.org/toc/apc/1160/1.

[28] A. Rich, J. V. House, D. W. Gidley, R. S. Conti, and P. W. Zitzewitz, Spin-polarized low-energy positron beams and their applications, Appl. Phys. A **43**, 275 (1987).

[29] D. W. Gidley, A. R. Köymen, and T. W. Capehart, Polarized Low-Energy Positrons: A New Probe of Surface Magnetism, Phys. Rev. Lett. **49**, 1779 (1982).

[30] D. Y. Ivanov, G. L. Kotkin, and V. G. Serbo, Complete description of polarization effects in emission of a photon by an electron in the field of a strong laser wave, Eur. Phys. J. C **36**, 127 (2004).

[31] D. Seipt and B. King, Spin- and polarization-dependent locally-constant-field-approximation rates for nonlinear compton and breit-wheeler processes, Phys. Rev. A **102**, 052805 (2020).

[32] T. N. Wistisen and A. Di Piazza, Numerical approach to the semiclassical method of radiation emission for arbitrary electron spin and photon polarization, Phys. Rev. D **100**, 116001 (2019).

[33] B. King and S. Tang, Nonlinear compton scattering of polarized photons in plane-wave backgrounds, Phys. Rev. A **102**, 022809 (2020).

[34] V. N. Baier, V. M. Katkov, A. I. Milshtein, and V. M. Strakhovenko, The theory of quantum processes in the field of a strong electromagnetic wave, Zh. Eksp. Teor. Fiz. **69**, 783 (1975) [Sov. Phys . JETP **42**, 400 (1975)], http://www.jetp.ras.ru/cgi-bin/dn/e_042_03_0400.pdf.

[35] S. Meuren and A. Di Piazza, Quantum Electron Self-Interaction in a Strong Laser Field, Phys. Rev. Lett. **107**, 260401 (2011).

[36] T. Podszus and A. Di Piazza, First-order strong-field QED processes including the damping of particle states, Phys. Rev. D **104**, 016014 (2021).

[37] A. Ilderton, B. King, and S. Tang, Loop spin effects in intense background fields, Phys. Rev. D **102**, 076013 (2020).

[38] G. Torgrimsson, Loops and polarization in strong-field QED, New J. Phys. **23**, 065001 (2021).

[39] G. Torgrimsson, Resummation of quantum radiation reaction and induced polarization, Phys. Rev. D **104**, 056016 (2021).

[40] D. Seipt, C. P. Ridgers, D. D. Sorbo, and A. G. R. Thomas, Polarized QED cascades, New J. Phys. **23**, 053025 (2021).

[41] R. D. Carlini, J. Finn, S. Kowalski, S. Page, D. Armstrong, A. Asaturyan, T. Averett, J. Benesch, J. Birchall, P. Bosted *et al.*, The qweak experiment: A search for new physics at the TeV scale via a measurement of the proton's weak charge, arXiv:1202.1255.

[42] S. Kowalski, Parity-violating electron scattering, HNPS Adv. Nucl. Phys. **15**, 2 (2020), https://eproceedings.epublishing.ekt.gr/index.php/hnps/article/viewFile/2614/pdf.

[43] D. T. Pierce and F. Meier, Photoemission of spin-polarized electrons from GaAs, Phys. Rev. B **13**, 5484 (1976).

[44] M. Swartz, Physics with polarized beams, Report No. SLAC-PUB-4656, 1988.

[45] H. Ohgaki, T. Noguchi, S. Sugiyama, T. Mikado, M. Chiwaki, K. Yamada, R. Suzuki, N. Sei, T. Ohdaira, and T. Yamazaki, Polarized gamma-rays with laser-Compton backscattering, Nucl. Instrum. Methods Phys. Res., Sect. A **375**, 602 (1996).

[46] T. Omori, M. Fukuda, T. Hirose, Y. Kurihara, R. Kuroda, M. Nomura, A. Ohashi, T. Okugi, K. Sakaue, T. Saito, J. Urakawa, M. Washio, and I. Yamazaki, Efficient Propagation of Polarization from Laser Photons to Positrons through Compton Scattering and Electron-Positron Pair Creation, Phys. Rev. Lett. **96**, 114801 (2006).

[47] D. Seipt, D. Del Sorbo, C. P. Ridgers, and A. G. R. Thomas, Theory of radiative electron polarization in strong laser fields, Phys. Rev. A **98**, 023417 (2018).

[48] G. L. Kotkin, V. G. Serbo, and V. I. Telnov, Electron (positron) beam polarization by Compton scattering on circularly polarized laser photons, Phys. Rev. ST Accel. Beams **6**, 011001 (2003).

[49] D. V. Karlovets, Radiative polarization of electrons in a strong laser wave, Phys. Rev. A **84**, 062116 (2011).

[50] A. Di Piazza, T. N. Wistisen, M. Tamburini, and U. I. Uggerhøj, Testing Strong Field QED Close to the Fully Nonperturbative Regime Using Aligned Crystals, Phys. Rev. Lett. **124**, 044801 (2020).

[51] T. Blackburn, A. Ilderton, M. Marklund, and C. Ridgers, Reaching supercritical field strengths with intense lasers, New J. Phys. **21**, 053040 (2019).

[52] C. Baumann, E. Nerush, A. Pukhov, and I. Y. Kostyukov, Probing non-perturbative QED with electron-laser collisions, Sci. Rep. **9**, 9407 (2019).

[53] A. M. Fedotov, Conjecture of perturbative QED breakdown at $\alpha\chi^{2/3} \gtrsim 1$, J. Phys. Conf. Ser. **826**, 012027 (2017).

[54] V. Yakimenko, S. Meuren, F. Del Gaudio, C. Baumann, A. Fedotov, F. Fiuza, T. Grismayer, M. J. Hogan, A. Pukhov, L. O. Silva, and G. White, Prospect of Studying Nonperturbative QED with Beam-Beam Collisions, Phys. Rev. Lett. **122**, 190404 (2019).

[55] A. A. Mironov, S. Meuren, and A. M. Fedotov, Resummation of QED radiative corrections in a strong constant crossed field, Phys. Rev. D **102**, 053005 (2020).

[56] V. Ritus, Radiative effects and their enhancement in an intense electromagnetic field, Zh. Eksp. Teor. Fiz. **57**, 2176 (1969) [Sov. Phys. JETP **30**, 1181 (1970)], http://jetp.ras.ru/cgi-bin/dn/e_030_06_1181.pdf.

[57] D. Hanneke, S. Fogwell, and G. Gabrielse, New Measurement of the Electron Magnetic Moment and the Fine Structure Constant, Phys. Rev. Lett. **100**, 120801 (2008).

[58] S. Sturm, A. Wagner, B. Schabinger, J. Zatorski, Z. Harman, W. Quint, G. Werth, C. H. Keitel, and K. Blaum, g Factor of Hydrogenlike $^{28}Si^{13+}$, Phys. Rev. Lett. **107**, 023002 (2011).

[59] B. Abi, T. Albahri, S. Al-Kilani, and *et al.* (Muon $g-2$ Collaboration), Measurement of the Positive Muon Anomalous Magnetic Moment to 0.46 ppm, Phys. Rev. Lett. **126**, 141801 (2021).

[60] C. Ridgers, J. Kirk, R. Duclous, T. Blackburn, C. Brady, K. Bennett, T. Arber, and A. Bell, Modelling gamma-ray photon emission and pair production in high-intensity lasermatter interactions, J. Comput. Phys. **260**, 273 (2014).

[61] N. V. Elkina, A. M. Fedotov, I. Y. Kostyukov, M. V. Legkov, N. B. Narozhny, E. N. Nerush, and H. Ruhl, QED cascades induced by circularly polarized laser fields, Phys. Rev. ST Accel. Beams **14**, 054401 (2011).

[62] A. Gonoskov, S. Bastrakov, E. Efimenko, A. Ilderton, M. Marklund, I. Meyerov, A. Muraviev, A. Sergeev, I. Surmin, and E. Wallin, Extended particle-in-cell schemes for physics in ultrastrong laser fields: Review and developments, Phys. Rev. E **92**, 023305 (2015).

[63] U. M. of CAIN Version 2.42, http://lcdev.kek.jp/~yokoya/CAIN/.

[64] V. I. Ritus, Quantum effects of the interaction of elementary particles with an intense electromagnetic field, J. Sov. Laser Res. **6**, 497 (1985).

[65] A. Di Piazza, M. Tamburini, S. Meuren, and C. H. Keitel, Implementing nonlinear Compton scattering beyond the local-constant-field approximation, Phys. Rev. A **98**, 012134 (2018).

[66] A. Di Piazza, M. Tamburini, S. Meuren, and C. H. Keitel, Improved local-constant-field approximation for strong-field QED codes, Phys. Rev. A **99**, 022125 (2019).

[67] A. Ilderton, B. King, and D. Seipt, Extended locally constant field approximation for nonlinear compton scattering, Phys. Rev. A **99**, 042121 (2019).

[68] Q. Z. Lv, E. Raicher, C. H. Keitel, and K. Z. Hatsagortsyan, Anomalous violation of the local constant field approximation in colliding laser beams, Phys. Rev. Research **3**, 013214 (2021).

[69] See Supplemental Material at http://link.aps.org/supplemental/10.1103/PhysRevLett.128.174801 for details on the applied theoretical model, simulated results for other laser and electron parameters, one-loop effects, and impact of laser polarization.

[70] V. N. Baier, V. M. Katkov, and V. S. Fadin, *Radiation from Relativistic Electrons* (Atomizdat, Moscow, 1973).

[71] Y. Tang, Z. Gong, J. Yu, Y. Shou, and X. Yan, Radiative polarization dynamics of relativistic electrons in an intense electromagnetic field, Phys. Rev. A **103**, 042807 (2021).

[72] V. B. Berestetskii, E. M. Lifshitz, and L. P. Pitaevskii, *Quantum Electrodynamics* (Pergamon, Oxford, 1982).

[73] G. Kotkin, H. Perlt, and V. Serbo, Polarization of high-energy electrons traversing a laser beam, Nucl. Instrum. Methods Phys. Res., Sect. A **404**, 430 (1998).
[74] L. H. Thomas, The kinematics of an electron with an axis, Philos. Mag. Ser. **3**, 1 (1927).
[75] V. Bargmann, L. Michel, and V. L. Telegdi, Precession of the Polarization of Particles Moving in a Homogeneous Electromagnetic Field, Phys. Rev. Lett. **2**, 435 (1959).
[76] M. Wen, H. Bauke, and C. H. Keitel, Identifying the stern-gerlach force of classical electron dynamics, Sci. Rep. **6**, 31624 (2016).
[77] M. Formanek, A. Steinmetz, and J. Rafelski, Motion of classical charged particles with magnetic moment in external plane-wave electromagnetic fields, Phys. Rev. A **103**, 052218 (2021).
[78] Y. I. Salamin, G. R. Mocken, and C. H. Keitel, Electron scattering and acceleration by a tightly focused laser beam, Phys. Rev. ST Accel. Beams **5**, 101301 (2002).
[79] A. Rich and J. C. Wesley, The current status of the lepton g factors, Rev. Mod. Phys. **44**, 250 (1972).
[80] See Sec. VI of the Supplemental Material [69] for the justification of the simplifications.